3.4. ULTRASTRUCTURE DE LA SPERMIOGENESE ET DU SPERMATOZOÏDE DE LA DOUVE DU FOIE *FASCIOLA HEPATICA* L., 1758 (DIGENEA, FASCIOLIDAE) : MICROSCOPIE ELECTRONIQUE A TRANSMISSION ET A BALAYAGE, ET IMMUNOCYTOCHIMIE DE LA TUBULINE

Résumé :

L'ultrastructure de la spermiogenèse et du spermatozoïde de *Fasciola hepatica* Linnaeus, 1758 (Trematoda, Digenea, Fasciolidae) est décrite en microscopie électronique à balayage (SEM) et à transmission (TEM). Chez *F. hepatica*, la spermiogenèse suit le modèle général déjà décrit chez les Digenea. Cependant, une rotation flagellaire d'environ 120º est décrite pour la première fois chez cette espèce et chez les Digenea. Le spermatozoïde mature de *F. hepatica* est une cellule filiforme d'environ 275 µm de long. La technique de « whole mount » et des observations au microscope électronique à balayage nous ont permis de démontrer la disposition spiralée des axonèmes le long du corps spermatique. Le spermatozoïde présente les mêmes caractéristiques ultrastructurales que *F. gigantica*. Les caractères les plus intéressants de ce gamète mâle sont les suivants : l'expansion cytoplasmique dorso-latérale, l'ornementation externe de la membrane cytoplasmique et les corps épineux. La localisation de la tubuline au niveau du cytosquelette microtubulaire de *F. hepatica* est aussi analysée au moyen d'anticorps monoclonaux (anti-α-tubuline, anti-β-tubuline, anti-α-tubuline acétylée et anti-α-tubuline tyrosinée). Ainsi les doublets des axonèmes et les microtubules corticaux sont marqués par ces anti-tubulines. Par contre, aucun de ces anticorps n'a permis le marquage de l'élément central de l'axonème 9 + '1' des Trepaxonemata.

Mots clés :

Ultrastructure, immunocytochimie, tubuline, spermiogenèse, spermatozoïde, *Fasciola hepatica*, Trematoda, Digenea, Fasciolidae

Acta Parasitologica, 2003, 48(3), 182–194; ISSN 1230-2821

Spermiogenesis and sperm ultrastructure of the liver fluke *Fasciola hepatica* L., 1758 (Digenea, Fasciolidae): transmission and scanning electron microscopy, and tubulin immunocytochemistry

Papa I. Ndiaye[1], Jordi Miquel[1]*, Roger Fons[2] and Bernard Marchand[3]

[1]Laboratori de Parasitologia, Departament de Microbiologia i Parasitologia Sanitàries, Facultat de Farmàcia, Universitat de Barcelona, Av. Joan XXIII, sn, E-08028 Barcelona, Spain; [2]Département d'Écologie Évolutive, Laboratoire Arago, CNRS UMR 7628, F-66650 Banyuls-sur-Mer, France; [3]Laboratoire Parasites et Écosystèmes Méditerranéens, Faculté des Sciences et Techniques, Université de Corse, F-20250 Corte, France

Abstract

We describe here the ultrastructure of spermiogenesis and the mature spermatozoon of *Fasciola hepatica* (Trematoda, Digenea, Fasciolidae) by means of scanning (SEM) and transmission electron microscopy (TEM). Spermiogenesis in *F. hepatica* follows the general pattern of digeneans. However, this is the first report of a flagellar rotation of about 120° in Digenea. The mature spermatozoon of *F. hepatica* is a filiform cell of about 275 μm in length. SEM and whole mount TEM revealed a helical pattern of axonemes around the sperm body. The spermatozoon presented the same ultrastructural organization as the congeneric *F. gigantica*. The most interesting features of the male gamete of *F. hepatica* therefore are the dorsolateral cytoplasmic expansion, the external ornamentation of the cell membrane and the spine-like bodies. We also analysed the distribution pattern of tubulin in the microtubular cytoskeleton of *F. hepatica* by means of monoclonal anti-tubulins (anti-α-tubulin, anti-β-tubulin, anti-α-acetylated tubulin and anti-α-tyrosinated tubulin). These anti-tubulins labelled axonemal and cortical microtubules but not the central core of the 9+'1' trepaxonematan axoneme.

Key words

Ultrastructure, SEM, TEM, immunocytochemistry, tubulin, spermiogenesis, spermatozoon, *Fasciola hepatica*, Digenea

Introduction

The liver fluke *Fasciola hepatica* L., 1758, is responsible for human fasciolosis, a major parasitic disease widely distributed throughout the world affecting some 2.4 million people while a further 180 million are at risk (Dalton 1999). Fasciolosis is also one of the most common parasitic diseases of domestic ruminants throughout the world, causing immense economic losses through herd mortality, liver failure, reduction in milk and meat production, etc. Several ultrastructural studies have been performed on species of the genus *Fasciola* (*F. hepatica* and *F. gigantica* Cobbold, 1856) (Gresson and Perry 1961; Stitt and Fairweather 1990, 1992; Srimuzipo *et al.* 2000; Dangprasert *et al*. 2001; Robinson *et al*. 2001; Meaney *et al*. 2002; Ndiaye *et al*. in press).

Here we compare the ultrastructural features of spermiogenesis and the spermatozoa of *F. hepatica* in a normal host (cattle, *Bos taurus*) and a natural reservoir in Corsica (black rat, *Rattus rattus*). The black rat and the mouse are new natural definitive hosts of *F. hepatica* on this island (Mas-Coma *et al*. 1988). Previous results from the ultrastructural study of spermatozoon of *F. hepatica* (Stitt and Fairweather 1990) differ considerably from those obtained for *F. gigantica* sperm (Ndiaye *et al*. in press). Therefore we compare here the results from the present study with previous observations on the sperm of the congeneric *F. gigantica* (Ndiaye *et al*. in press) and provide a complete description of ultrastructural characters of *F. hepatica* sperm by means of SEM and TEM.

We also analysed the distribution pattern of tubulin in the microtubular cytoskeleton by means of monoclonal anti-tubu-

*Corresponding author: jordimiquel@ub.edu

lins (anti-α-tubulin, anti-β-tubulin, anti-α-acetylated tubulin and anti-α-tyrosinated tubulin). To date, only 10 species of Platyhelminthes, including acoels, temnocephalids, monogeneans, digeneans and cestodes, have been the subject of immunocytochemical studies of tubulin distribution in sperm (Iomini *et al*. 1995, Iomini and Justine 1997, Mollaret and Justine 1997, Justine *et al*. 1998, Justine 1999, Miquel and Marchand 2001). The present study is the first assess to the labelling of tyrosinated tubulin by means of TEM.

Materials and methods

Materials

Living specimens of *F. hepatica* were collected from the liver of cattle (*Bos taurus*) from several localities of Cerdanya (Catalonia, Spain) and from infected black rats (*Rattus rattus*) in the mouth of the Fango river (Galéria, Corsica island, Mediterranean Sea). Living flukes were placed in 0.9% NaCl solution and dissected in order to isolate portions containing testes and seminal ducts.

Transmission electron microscopy (*TEM*)

Sections containing testes and seminal ducts were fixed at 4°C in 2.5% glutaraldehyde in 0.1 M sodium cacodylate buffer at pH 7.4 for 2 h, rinsed in sodium cacodylate buffer and post-fixed in 1% osmium tetroxide in the same buffer for 1 h at 4°C. Next they were rinsed in sodium cacodylate buffer, dehydrated in ethanol solutions and propylene oxide, embedded in Spurr's resin, and polymerised at 60°C for 48 h. Ultrathin sections (50–60 nm) were cut on a Reichert-Jung Ultracut E ultramicrotome, placed on 200-mesh copper grids and stained with uranyl acetate and lead citrate, following Reynolds (1963). The grids were examined using an Hitachi H-600 electron microscope at 75 kV.

In addition, seminal ducts were dissected in 0.9% NaCl solution in order to isolate mature spermatozoa. Thus, one drop of the solution was placed between slide and cover slide and then stained with 0.5% blue methyl solution and 0.5% borax to measure spermatozoon length. The other part of this solution was fixed with 2.5% glutaraldehyde in 0.1 M phosphate buffer at 4°C overnight. It was then rinsed with phosphate buffer and post-fixed for 2 h in 1% osmium tetroxide solution in the same buffer at 4°C and treated following the whole mount technique. Finally, after rinsing with distilled water, samples were mounted on 400-mesh copper grids for observation using an Hitachi H-800 transmission electron microscope at 150–200 kV.

Scanning electron microscopy (*SEM*)

A solution containing living spermatozoa was fixed in 2.5% glutaraldehyde in 0.1 M phosphate buffer at pH 7.4 at 4°C, rinsed in phosphate buffer and post-fixed in 1% osmium tetroxide in the same buffer. After the last wash with distilled water, samples were mounted in poly-L-lysine, dehydrated in a progressive ethanol series and critical-point dried. Spermatozoa were finally sputter-coated with gold and observed in a Leica LC-360 scanning electron microscope at 10 kV.

Tubulin immunocytochemistry

Portions of material containing testes and seminal ducts of living fluke were fixed in cold (4°C) 4% paraformaldehyde and 0.25% glutaraldehyde in a 0.1 M sodium cacodylate buffer at pH 7.4 for 4 h, PLT [progressive lowering of temperature (–35°C)] dehydrated with a progressive series of ethanol, embedded in Lowicryl K4M, and UV polymerized at –35°C. Ultrathin sections were cut on a Reichert-Jung Ultracut E ultramicrotome and placed on gold grids. Non-specific antigens were blocked with 1% bovine serum albumin (BSA, Sigma A-7638) and 20 nM glycine (Sigma G-7126) in 0.1 M phosphate buffer saline (PBS) at pH 7.4 for 30 min at room temperature. A monoclonal anti-α-tubulin (clone NS-1 × Balb/C_{57} spleen cells, Amersham N-356), anti-β-tubulin (clone TUB 2.1, mouse ascites fluid, Sigma T-40266), anti-acetylated tubulin (clone 6-11 B-1, mouse ascites fluid, Sigma T-6793) and anti-tyrosine tubulin (clone TUB-1A2, mouse ascites fluid, Sigma T-9028) antibodies diluted at 1/50, 1/2, 1/10, and 1/10, respectively in 1% BSA in 0.1 M PBS at pH 7.4 were applied for 2 h at room temperature. After rinsing (1% BSA in 0.1 M PBS at pH 7.4, 3 × 5 min), a gold-conjugated antibody (goat anti-mouse, 15 nm gold, British Biocell EM-GAM 15), diluted at 1/25 in 1% BSA in 0.1 M PBS at pH 7.4, was applied for 1 h at room temperature. Controls were done by omitting the first antibody. After a final rinse (4 × 5 min in 0.1 M PBS at pH 7.4, 4 × 5 min in distilled water, and jet-wash), the grids were dried on Whatman paper, stained with uranyl acetate (10 min) and lead citrate (3 min), and observed in a Jeol 1010 electron microscope at 80 kV.

Results

Spermiogenesis (Figs 1–8)

Spermiogenesis of *F. hepatica* begins with the formation of a differentiation zone in the spermatid. This is a conical area that contains two centrioles outbided by striated rootlets and separated by an intercentriolar body (Figs 1 and 2). Each centriole develops a flagellum which grows externally to a median cytoplasmic expansion that develops at the base of the differentiation zone (Fig. 3). Later, asynchronic rotation of the two free flagella occurs. These become parallel to the median cytoplasmic expansion with which they fuse (Figs 3–5). The flagellar rotation is 120° at least for one of them (Fig. 3). Electron-dense areas were observed on the internal face of the cytoplasmic membrane of the median cytoplasmic expansion

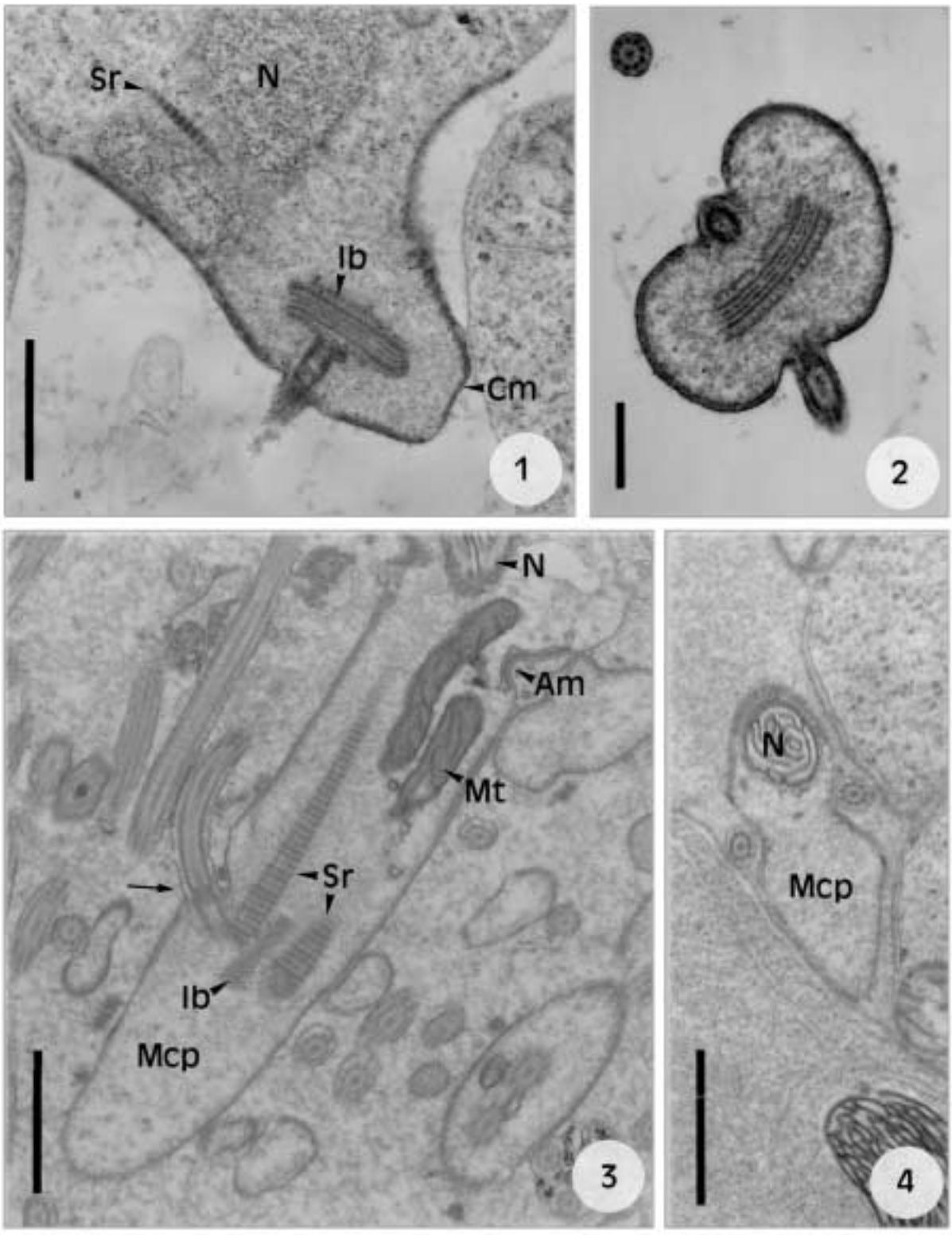

Figs 1–4. Spermiogenesis in *Fasciola hepatica*, TEM micrographs: **1.** Initial stage of spermiogenesis showing a differentiation zone; scale bar = 1 µm. **2.** Detail of intercentriolar body; scale bar = 0.5 µm. **3.** Zone of differentiation showing the 120° of the free flagellum (arrow); scale bar = 1 µm. **4.** Cross-section of a spermatid showing the nuclear migration before the proximodistal fusion of the free flagella; scale bar = 1 µm. **Abbreviations to all figures:** Am – arched membranes, Ase – anterior spermatozoon extremity, Ax – axonemes, Cm – cortical microtubules, D – doublets, Edl – dorsolateral cytoplasmic expansion, Eo – external ornamentation of the cell membrane, G – glycogen, Ib – intercentriolar body, Mcp – median cytoplasmic process, Mt – mitochondrion, N – nucleus, Pse – posterior spermatozoon extremity, Sb – spine-like body, Sr – striated root

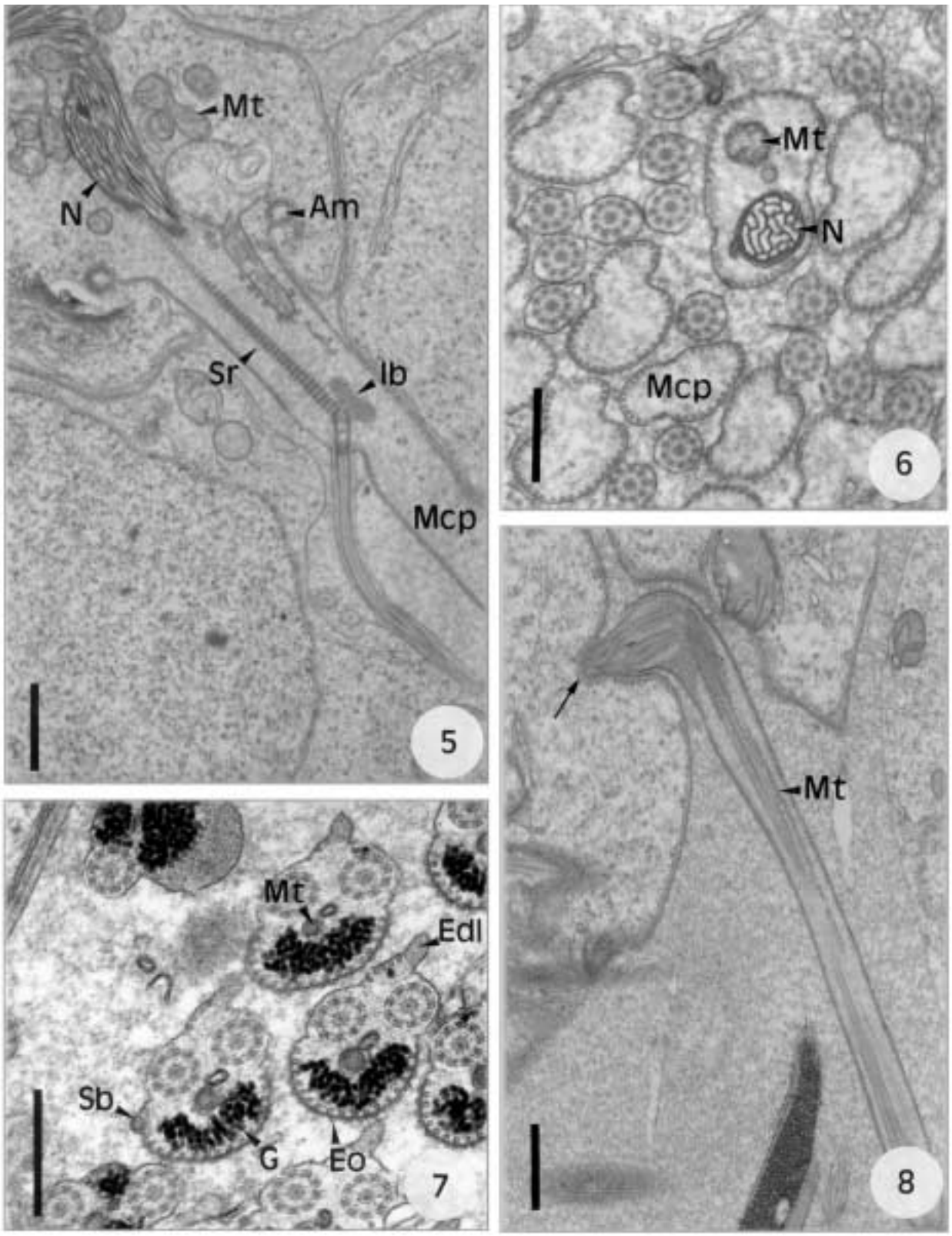

Figs 5–8. Spermiogenesis in *Fasciola hepatica*, TEM micrographs: **5.** Longitudinal section of a zone of differentiation showing the initial migration of the nucleus and the mitochondrion; scale bar = 1 µm. **6.** Diverse cross-sections of the median cytoplasmic process; scale bar = 0.5 µm. **7.** Cross-sections of spermatids in an advanced stage of spermiogenesis. Note the presence of the dorsolateral cytoplasmic expansion, the spine-like body and the external ornamentation of the membrane; scale bar = 0.5 µm. **8.** Longitudinal section of a spermatid in a final stage of spermiogenesis. The ring of arched membranes is strangled (arrow); scale bar = 1 µm

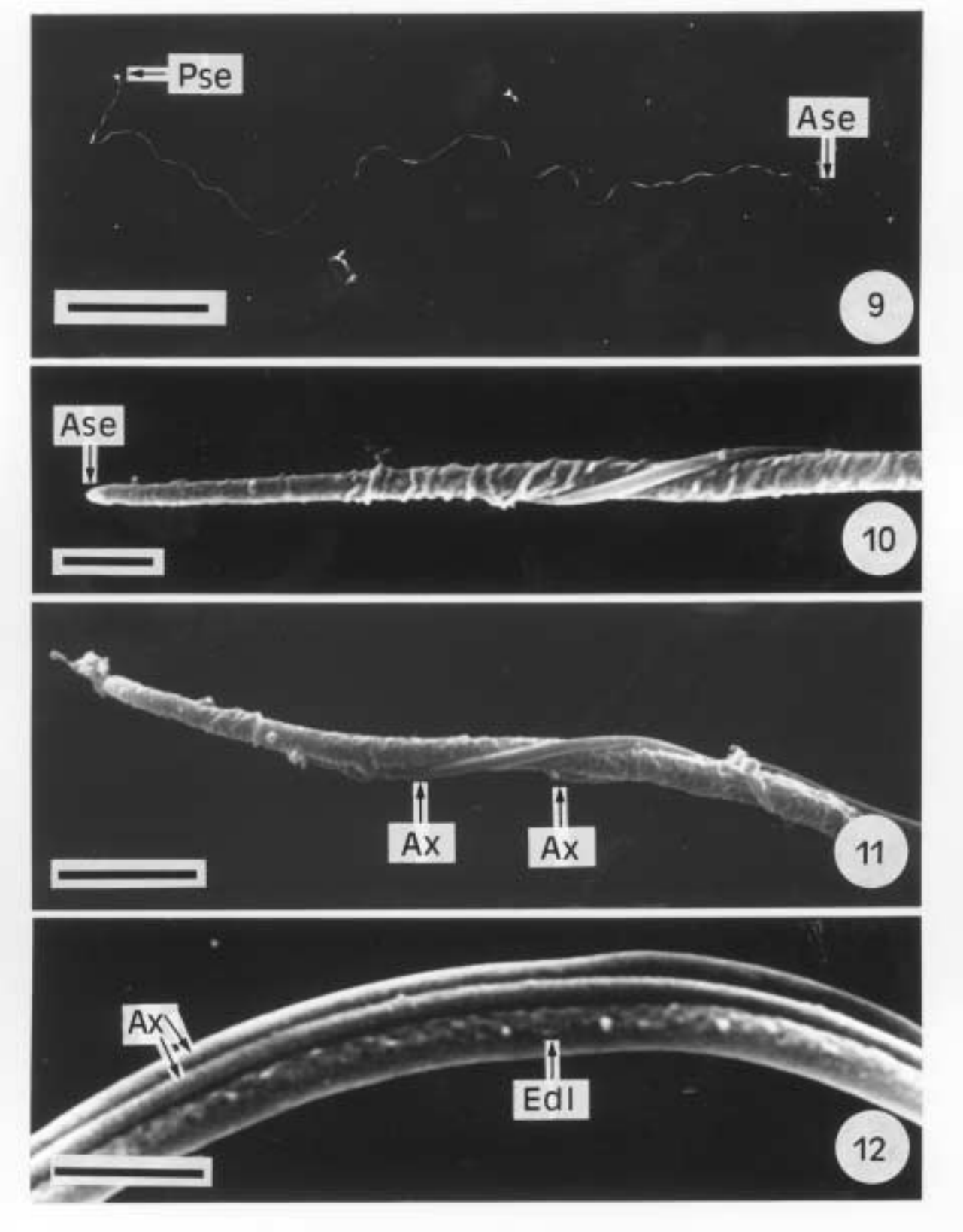

Figs 9–12. Mature spermatozoon of *Fasciola hepatica*, SEM micrographs: **9.** Whole spermatozoon; scale bar = 50 µm. **10.** Anterior extremity of the spermatozoon showing a single axoneme; scale bar = 1 µm. **11.** Anterior extremity of the spermatozoon showing the two axonemes; scale bar = 2 µm. **12.** Region of spermatozoon with the presence of the dorsolateral cytoplasmic expansion; scale bar = 1 µm

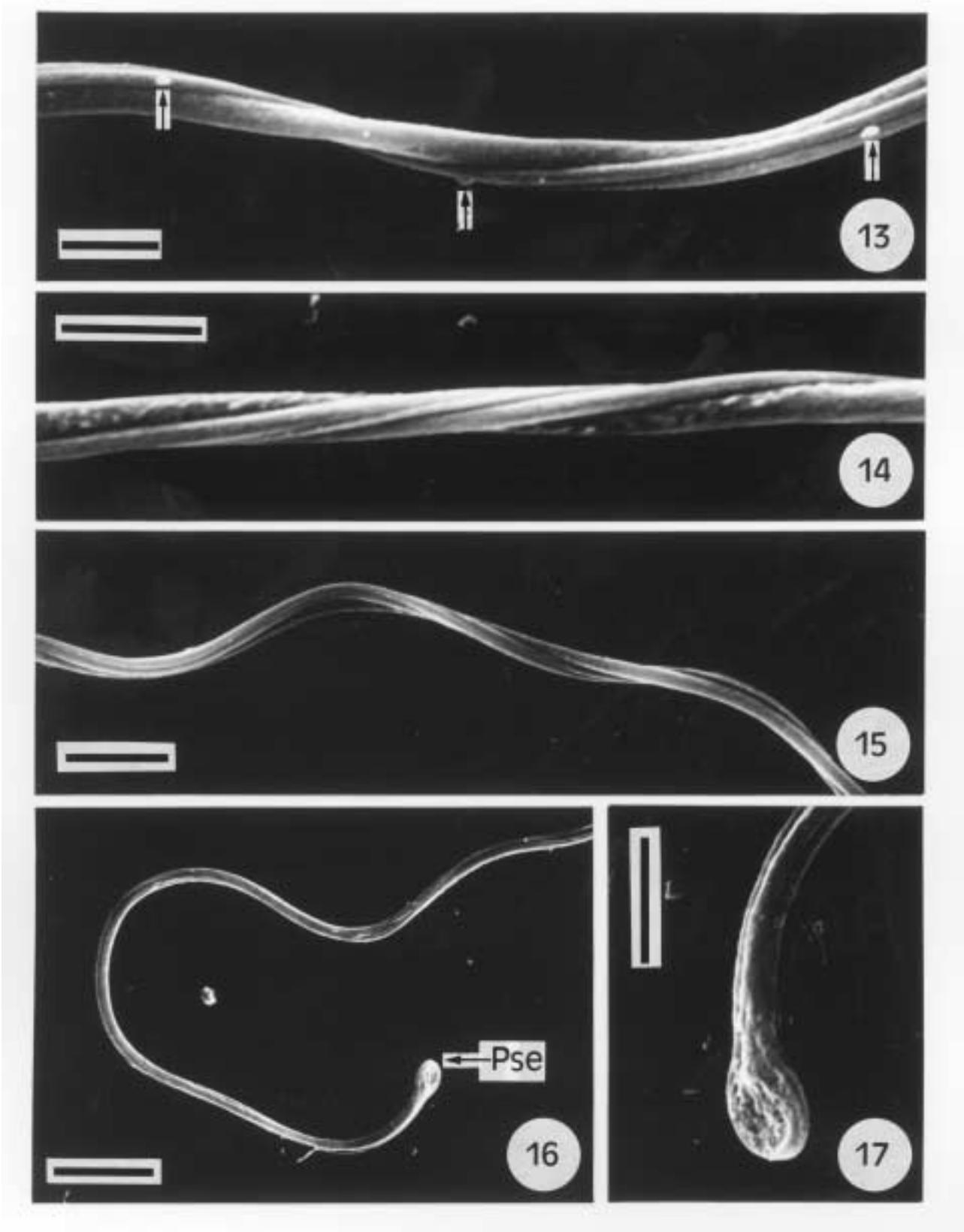

Figs 13–17. Mature spermatozoon of *Fasciola hepatica*, SEM micrographs: **13.** Region of the mature sperm showing the spine-like bodies (arrows); scale bar = 1 µm. **14.** Mitochondrial region of the spermatozoon showing the helical pattern of axonemes; scale bar = 1 µm. **15.** Region showing the helical pattern of the spermatozoon. Scale bar = 2 µm. **16.** Posterior extremity of the spermatozoon; scale bar = 5 µm. **17.** Detail of the posterior tip of the spermatozoon; scale bar = 2 µm

just before the proximodistal fusion and separate the submembranous layer of cortical microtubules in two sets on the ventral and dorsal faces of the spermatid (Fig. 6). Nuclear and mitochondrial migrations toward the median cytoplasmic expansion occur in the early stage of spermiogenesis (before the proximodistal fusion) (Figs 4 and 6). In the final stage of spermiogenesis, we observed the simultaneous presence of a dorsolateral cytoplasmic expansion, an external ornamentation of the plasma membrane and spine-like bodies (Fig. 7). The presence of these three structures was also observed in cross-sections of the anterior part of the spermatozoon. Spermiogenesis ends when the ring of arched membranes is constricted (Fig. 8) and the young spermatozoon is released from the residual cytoplasm.

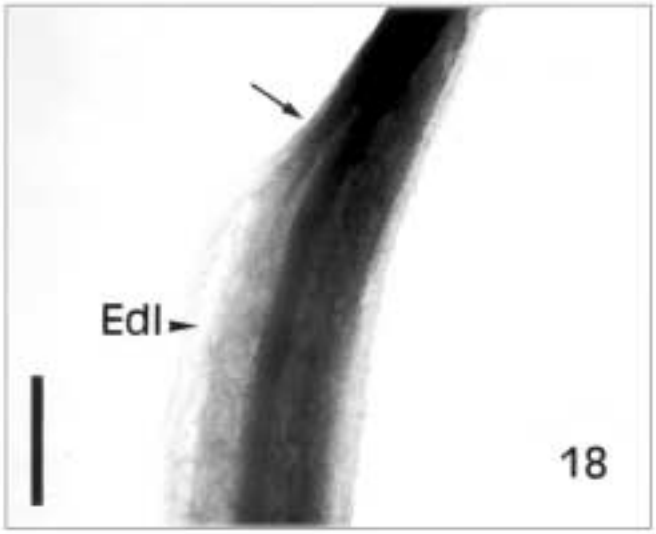

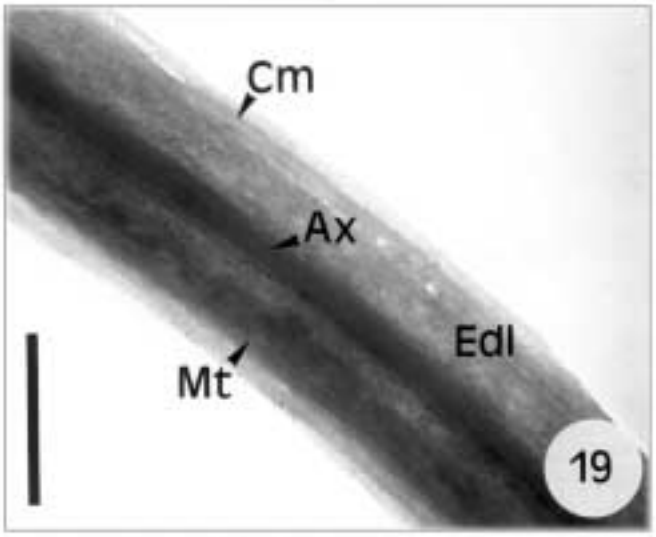

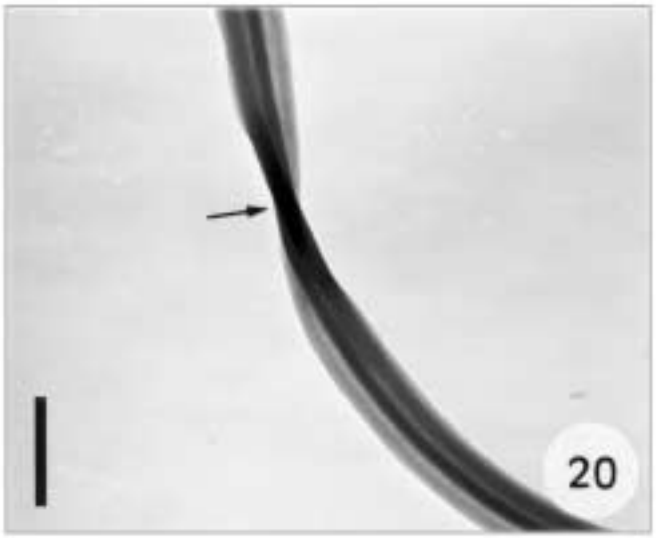

Spermatozoon (Figs 9–28)

SEM shows that the spermatozoon of *F. hepatica* has a long filiform cell (Fig. 9) that measures approximately 275 μm in length. Observations of various transverse and longitudinal sections of the spermatozoon by TEM reveal two axonemes, a nucleus, a mitochondrion, two sets of parallel cortical microtubules and other ultrastructural features that characterize this species. Both SEM and TEM micrographs reveal a single axoneme in the anterior extremity of sperm (Figs 9–11, 21). Later, a hook-shaped dorsolateral cytoplasmic expansion is observed (Figs 12, 18, 19, 21, 24) in a region that contains two axonemes. In this area, the cortical microtubules are regularly spaced except in the dorsolateral cytoplasmic expansion, where they are closer together on the ventral face (Figs 21 and 24). In this region, we counted 35 to 45 cortical microtubules that form a continuous submembranous layer. Therefore, the anterior region of the spermatozoon is characterized by the three structures described in final stage of spermiogenesis (i.e. the dorsolateral cytoplasmic expansion, the external ornamentation of the cell membrane and the spine-like bodies) (Figs 12, 13, 18, 19, 21, 24–26). Cross-sections of the mitochondrial region of the spermatozoon reveal a progressive disappearance of the cytoplasmic expansion and the external ornamentation of the cell membrane (Figs 24–26). The disappearance of the latter is associated with stacking of cortical microtubules (Fig. 28). Spine-like bodies were observed only in the anterior areas of the sperm (Figs 25 and 26). The internal and electron-dense spherical vesicle is around 50 nm in diameter. SEM and whole mount TEM clearly demonstrated that, in certain areas of sperm, the axonemes are twisted in a helical disposition along the spermatozoon (Figs 10, 11, 13–16, 20). The middle region of sperm contains two axo-

Figs 18–20. Mature spermatozoon of *F. hepatica*, whole mount technique, TEM micrographs: **18.** Anterior region of spermatozoon showing the beginning (arrow) of the dorsolateral cytoplasmic expansion; scale bar = 0.5 μm. **19.** Area of spermatozoon containing dorsolateral cytoplasmic expansion and mitochondrion; scale bar = 0.5 μm. **20.** Area of spermatozoon showing the twisted pattern of axonemes (arrow); scale bar = 1 μm

Table I. Comparison of available data of immunocytochemical labelling of spermatozoon microtubules of Platyhelminthes

Groups and species of Platyhelminthes	Labelling of spermatozoon microtubules												References
	axonemal microtubules				cortical microtubules				central core of 9+'1' axoneme				
	α	β	acetyl.	tyrosin.	α	β	acetyl.	tyrosin.	α	β	acetyl.	tyrosin.	
Acoela													
Actinoposthia beklemischevi	+	+	+		+	+	+		Np	Np	Np	Np	Justine *et al.* (1998), Raikova *et al.* (1998), Justine (1999)
Symsagittifera schultzei	+	+	+		Np	Np	Np	Np	Np	Np	Np	Np	Raikova *et al.* (1998)
Symsagittifera psammophila	+	+	+		Np	Np	Np	Np	Np	Np	Np	Np	Raikova *et al.* (1998)
Convoluta saliens	+	+	+		Np	Np	Np	Np	Np	Np	Np	Np	Justine (1999), Raikova and Justine (1999)
Temnocephalida													
Troglocaridicola sp.	+	+	+		+	+	–		–	–	–		Justine *et al.* (1998), Justine (1999)
Monogenea													
Pseudodactylogyrus sp.	+	+	+		Np	Np	Np	Np	–	–	–		Mollaret and Justine (1997), Justine *et al.* (1998), Justine (1999)
Digenea													
Echinostoma caproni	+	+	+		+	+	–		–	–	–		Iomini *et al.* (1995), Justine *et al.* (1998), Justine (1999)
Echinostoma liei	+	+	+		+	+	–		–	–	–		Iomini *et al.* (1995)
Fasciola hepatica	+	+	+	+	+	+	+	+	–	–	–	–	Present study
Cestoda													
Mesocestoides litteratus	+	+	+		+	+	+		–	–	–		Miquel and Marchand (2001)

Acetyl. – acetylated, tyrosin. – tyrosinated, (+) – labelling, (–) – no labelling, Np – structure not present in considered species.

nemes, a mitochondrion and a nucleus (Fig. 22). Cross-sections in the posterior areas of sperm show two axonemes and a well-developed nucleus (Fig. 27). In a posterior area of sperm, we detected the disorganization of the first axoneme in the nuclear region (Figs 22 and 28). Later, the disruption of the second axoneme occurs and the posterior extremity of the spermatozoon contains only a large nucleus (Figs 17 and 22). Large amounts of glycogen granules were observed in the mature sperm (Figs 22, 23, 26–28).

Tubulin immunocytochemistry (Figs 29–37)

Results of the immunolocalization of tubulin in the microtubular cytoskeleton of the spermatozoon of *F. hepatica* are shown in Table I. The axonemal microtubules and cortical microtubules of *F. hepatica* spermatids and mature spermatozoa show the same pattern of labelling by the antibodies. Thus, all the tubulins tested (α-tubulin, β-tubulin, acetylated tubulin and tyrosinated tubulin) labelled the two types of microtubules (axonemal and cortical) (Figs 29–37). In contrast, none of the anti-tubulin antibodies labelled the central core of the 9+'1' axoneme of trepaxonematan Platyhelminthes (Figs 31–37).

Discussion

Spermiogenesis and spermatozoon ultrastructure

Here we have observed the same pattern of spermiogenesis and the same ultrastructural characters in the spermatozoon of the liver fluke *F. hepatica* from the black rat *R. rattus* from the mouth of the Fango river in Corsica and from cattle from several localities of Cerdanya (Catalonia, Spain). Furthermore, other species of the genus *Fasciola* (*F. gigantica*) also show similar ultrastructural features (Ndiaye *et al*. in press).

Spermiogenesis in *F. hepatica* follows the general pattern described in all digenetic trematodes studied to date (e.g. Burton 1972; Grant *et al*. 1976; Ress 1979; Hendow and James 1988; Castilho and Barandela 1990; Iomini and Justine 1997; Miquel *et al*. 2000; Baptista-Farias *et al*. 2001; Ndiaye *et al*. 2002, 2003, in press). Nevertheless, here we report on an original aspect in the spermiogenesis of a digenean platyhelminth for the first time, namely the rotation of about 120° of at least one of the two free flagella with respect to the spermatid axis.

The mature spermatozoon of *F. hepatica* shows the same ultrastructural organization as the congeneric species *F. gi-*

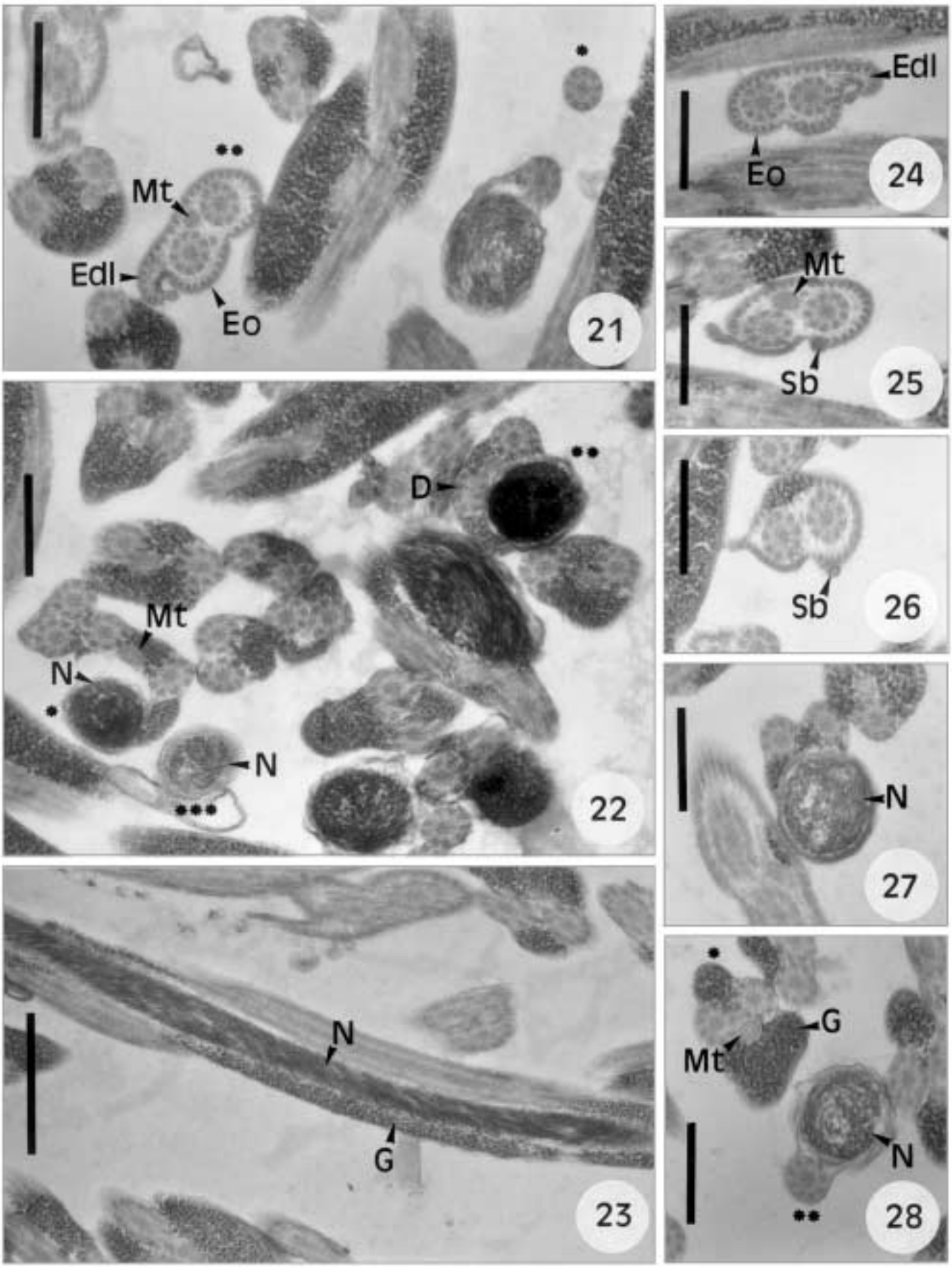
Mt
Edl
Eo
21
D
Mt
N
N
22
N
G
23
Edl
Eo
24
Mt
Sb
25
Sb
26
N
27
G
Mt
N
28

gantica (Ndiaye *et al*. in press): (a) a single axoneme in the anterior extremity of sperm; (b) the simultaneous presence of dorsolateral cytoplasmic expansion, external ornamentation of the gamete membrane and spine-like bodies; (c) a biflagellate area of the gamete containing firstly mitochondrion, later mitochondrion plus nucleus, and finally only nucleus; (d) the progressive disruption of the mitochondrion, later the first axoneme, and after the second; and (e) the posterior end of gamete with only the nucleus.

The presence of an external ornamentation of the plasma membrane in the male gamete of digeneans has been described previously; this ultrastructural character is present in the mature sperm of 14 species that belong to 13 families. These are *Scaphiostomum palaearcticum* (Brachylaimidae) (Ndiaye *et al*. 2002), *Bucephaloides gracilescens* and *Pseudorhipidocotyle elpichthys* (Bucephalidae) (Erwin and Halton 1983, Tang *et al*. 1998), *Neochasmus* sp. (Cryptogonimidae) (Jamieson and Daddow 1982), *Gonapodasmius* sp. (Didymozoidae) (Justine and Mattei 1982a), *Echinostoma caproni* (Echinostomatidae) (Iomini and Justine 1997), *F. gigantica* (Fasciolidae) (Ndiaye *et al*. in press), *Proctoeces maculatus* (Fellodistomidae) (Justine 1995), *Haematoloechus* sp. (Haematoloechidae) (Justine and Mattei 1982b), *Postorchigenes gymnesicus* (Lecithodendriidae) (Gracenea *et al*. 1997), *Notocotylus neyrai* (Notocotylidae) (Ndiaye *et al*. 2003), *Opecoeloides furcatus* (Opecoelidae) (Miquel *et al*. 2000), *Aphalloides coelomicola* (Opisthorchiidae) (Justine 1995) and *Paragonimus ohirai* (Paragonimidae) (Orido 1988).

In addition, *F. gigantica* (Ndiaye *et al*. in press) and *F. hepatica* have a hook-shaped dorsolateral cytoplasmic expansion. Several digeneans show cytoplasmic expansions in spermatozoa (*B. gracilescens* – Erwin and Halton 1983, or *S. palaearcticum* – Ndiaye *et al*. 2002); however, a hook-shaped expansion has previously been described only in *E. caproni* (Echinostomatidae) (Iomini and Justine 1997) and in *F. gigantica* (Ndiaye *et al*. in press). In these three species there are around 40 cortical microtubules in the area with the maximum development of the hook-shaped cytoplasmic expansion. At this level a difference in the location of the mitochondrion in the mature sperm of *E. caproni* and *Fasciola* spp. is observed. In all the three species this hook-shaped region of the spermatozoon contains the anterior extremity of the mitochondrion, but in *E. caproni* it is situated in the cytoplasmic expansion (Iomini and Justine 1997). In contrast, in *F. gigantica* (Ndiaye *et al*. in press) and *F. hepatica* this extremity is located between the two axonemes on the dorsal face of sperm.

Spine-like bodies were described for the first time by Miquel *et al*. (2000) in the fish parasite *O. furcatus* (Opecoelidae). They were later observed in the notocotylid *N. neyrai* (Ndiaye *et al*. 2003) and in *F. gigantica* (Ndiaye *et al*. in press). In *O. furcatus* and *F. gigantica* (Miquel *et al.* 2000, Ndiaye *et al.* in press) the periodicity of this character was evaluated as 1 μm in the mitochondrial area of sperm. We also observed this structure in the spermatozoon of *F. hepatica*, but in this species the distance between the spine-like bodies was larger and irregular. These bodies consisted of prominent and submembranar structures containing an electron-dense and spherical vesicle, the latter measuring around 50 nm in diameter in all four species (*O. furcatus*, *N. neyrai*, *F. gigantica* and *F. hepatica*).

SEM analysis of the spermatozoon of *F. hepatica* showed a helical disposition of the axonemes around the sperm body as has been found in *P. ohirai* (Orido 1988, Hirai and Tada 1991) and *E. caproni* (Iomini and Justine 1997) spermatozoa. This helical pattern, which is easily observed by means of SEM and whole mount TEM, it is not clearly shown in the longitudinal and transverse sections using TEM. Consequently, in certain areas of the gamete the helical disposition of axonemes around the spermatozoon body is probably more frequent than available studies show.

The results from previous ultrastructural studies of *F. hepatica* sperm development (Stitt and Fairweather 1990) differ considerably from our observations. Those authors describe the presence of two mitochondria and a posterior extremity of the male gamete with two axonemes firstly and with a single axoneme posteriorly. In this regard, according to Stitt and Fairweather (1990) the nucleus does not constitute the posterior end of the sperm. In contrast, in our observations on *F. hepatica* as well as those on *F. gigantica* (Ndiaye *et al*. in press), a single mitochondrion and a posterior extremity constituted by the nucleus were observed. Moreover, Stitt and Fairweather (1990) did not describe the dorsolateral cytoplasmic expansion or the external ornamentation of the plasma membrane. Nevertheless, an electron micrograph of the mitochondrial area of the spermatozoon shows an external ornamentation around the gamete. Since the transition between two mitochondria was not observed in any longitudinal section, the hypothesis that there were two mitochondria was based on the observation of a large number of cross-sections. In our opinion, the observation of more than one mitochondrion in the spermatozoon of several digenean species (*Haematoloechus medioplexus* by Burton 1972, *Pharyngosto-*

Figs 21–28. Mature spermatozoon of *F. hepatica*, TEM micrographs: **21.** Cross-sections of anterior area of the spermatozoon with single (*) and two axonemes (**); scale bar = 0.5 μm. **22.** Cross-sections of the nuclear area of the spermatozoon (*, ** and ***). Note the presence of only the nucleus in the posterior areas of the spermatozoon (***); scale bar = 0.5 μm. **23.** Longitudinal section of the nuclear region of the spermatozoon; scale bar = 1 μm. **24.** Cross-section of anterior area of the spermatozoon showing the dorsolateral cytoplasmic expansion and the external ornamentation of the cell membrane; scale bar = 0.5 μm. **25.** Cross-section of anterior area of the spermatozoon showing the mitochondrion and the spine-like body; scale bar = 0.5 μm. **26.** Another cross-section of anterior area of the spermatozoon with spine-like body; scale bar = 0.5 μm. **27.** Cross-section of the nuclear area of the spermatozoon; scale bar = 0.5 μm. **28.** Cross-sections of mitochondrial (*) and nuclear (**) areas of the spermatozoon; scale bar = 0.5 μm

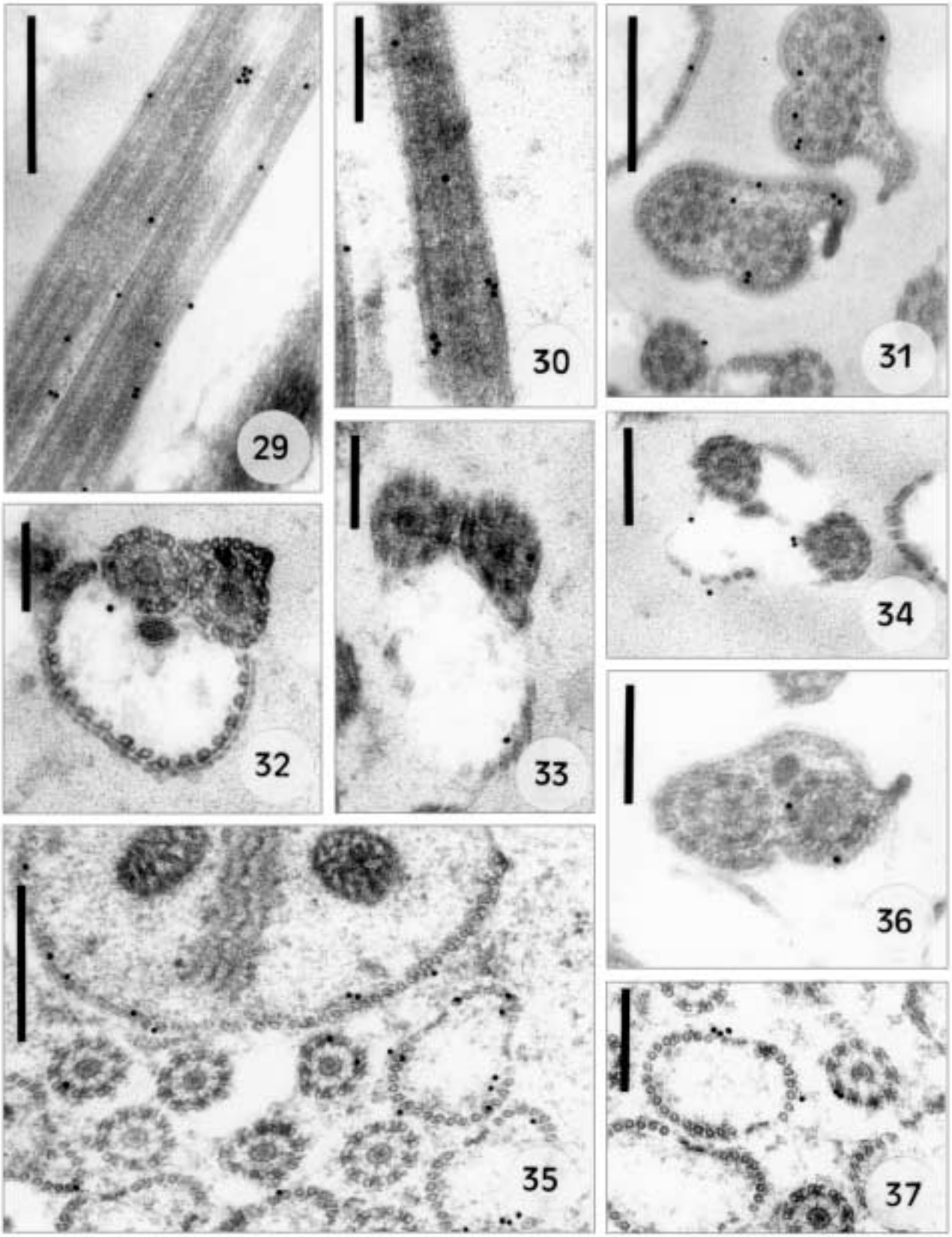
29
30
31
32
33
34
35
36
37

moides procyonis by Grant *et al*. 1976, *Cryptocotyle lingua* by Rees 1979, *Paragonimus ohirai* by Orido 1988, *Maritrema linguilla* by Hendow and James 1988, *Dicrocoelium dendriticum* by Cifrián *et al*. 1993, *F. hepatica* by Stitt and Fairweather 1990, *Postorchigenes gymnesicus* by Gracenea *et al*. 1997, *N. neyrai* by Ndiaye *et al*. 2003) may indicate a late fusion (when the spermatozoon is already formed) of the multiple mitochondria that migrate into the spermatid body. Regarding the posterior extremity of the spermatozoon of *F. hepatica*, here we show that this posterior end is widened, lacks an axoneme and is constituted by a large nucleus.

Tubulin immunocytochemistry

In Table I we show the results of the immunocytochemical study of the distribution of tubulin in the microtubular cytoskeleton of the sperm of *F. hepatica* coming from the black rat. Both axonemal and cortical microtubules showed the same pattern of labelling by the antibodies in the *F. hepatica* sperm collected from black rats. Our results on α-tubulin, β-tubulin and acetylated-α-tubulin are similar to those observed in other Platyhelminthes such as the acoel *Actinoposthia beklemischevi* (Justine 1999) and the cestode *Mesocestoides litteratus* (Miquel and Marchand 2001). All α-tubulin, β-tubulin, acetylated-α-tubulin and tyrosinated-α-tubulin tested here were labelled in axonemal and cortical microtubules. In contrast, none of the anti-tubulin antibodies labelled the central core of the 9+'1' trepaxonematan axoneme. These results are consistent with the findings of other studies [Iomini *et al*. (1995), Iomini and Justine (1997), Mollaret and Justine (1997), Justine *et al*. (1998), Justine (1999), and Miquel and Marchand (2001)] in *Troglocaridicola* sp., in the species of the genus *Echinostoma* and in *Mesocestoides litteratus* for α-tubulin, β-tubulin and acetylated-α-tubulin. The observation that anti-tyrosinated-α-tubulin did not label the central core of the 9+'1' axoneme increases the immunocytochemical data that supports the particular composition of the central structure of the trepaxonematan axoneme.

Acknowledgements. We thank the "Serveis Cientificotčcnics" of the University of Barcelona for their support in the preparation of materials. We also thank the "Servicio de Inspección Sanitaria de Mercados Centrales (Escorxador de Mercabarna)" for providing the cattle livers. This study was partially supported by the Spanish projects 2001-SGR-00088 from the "Comissionat per a Universitats i Recerca" and HF2002-0063 from the "Ministerio de Ciencia y Tecnología", and by a fellowship from the "Agencia Española de Cooperación Internacional – AECI" of the "Ministerio de Asuntos Exteriores" of Spain granted to Papa Ibnou Ndiaye.

References

Baptista-Farias M.F.D., Kohn A., Cohen S.C. 2001. Ultrastructure of spermatogenesis and sperm development in *Saccocoeloides godoyi* Kohn & Froes, 1986 (Digenea, Haploporidae). *Memórias do Instituto Oswaldo Cruz*, 96, 61–70.

Burton P.R. 1972. Fine structure of the reproductive system of a frog lung fluke. III. The spermatozoon and its differentiation. *Journal of Parasitology*, 58, 68–83.

Castilho F., Barandela T. 1990. Ultrastructural study on the spermiogenesis and spermatozoon of the metacercariae of *Microphallus primas* (Digenea), a parasite of *Carcinus maenas*. *Molecular Reproduction and Development*, 25, 140–146.

Cifrián B., García-Corrales P., Martínez-Alós S. 1993. Ultrastructural study of the spermatogenesis and mature spermatozoa of *Dicrocoelium dendriticum* (Plathelminthes, Digenea). *Parasitology Research*, 79, 204–212.

Dalton J.P. 1999. Fasciolosis. CABI Publishing, New York.

Dangprasert T., Khabsuk W., Meepool A., Wanichanon C., Viyanant V., Upatham E.S., Wongratanacheevin S., Sobhon P. 2001. *Fasciola gigantica*: surface topography of the adult tegument. *Journal of Helminthology*, 75, 43–50.

Erwin B.E., Halton D.W. 1983. Fine structural observations on spermatogenesis in a progenetic trematode, *Bucephaloides gracilescens*. *International Journal for Parasitology*, 13, 413–426.

Gracenea M., Ferrer J.R., González-Moreno O., Trullols M. 1997. Ultrastructural study of spermatogenesis and spermatozoon in *Postorchigenes gymnesicus* (Trematoda, Lecithodendriidae). *Journal of Morphology*, 234, 223–232.

Grant W.C., Harkema R., Muse K.E. 1976. Ultrastructure of *Pharyngostomoides procyonis* Harkema 1942 (Diplostomatidae). I. Observations on the male reproductive system. *Journal of Parasitology*, 62, 39–49.

Gresson R.A.R., Perry M.M. 1961. Electron microscope studies of spermateleosis in *Fasciola hepatica* L. *Experimental Cell Research*, 22, 1–8.

Hendow H.T., James B.L. 1988. Ultrastructure of spermatozoon and spermatogenesis in *Maritrema linguilla* (Digenea: Microphallidae). *International Journal for Parasitology*, 18, 53–63.

Hirai H., Tada I. 1991. Morphological features of spermatozoa of *Paragonimus ohirai* (Trematoda: Platyhelminthes) examined by a silver nitrate staining technique. *Parasitology*, 103, 103–110.

Iomini C., Justine J.-L. 1997. Spermiogenesis and spermatozoon of *Echinostoma caproni* (Platyhelminthes, Digenea): transmission and scanning electron microscopy, and tubulin immunocytochemistry. *Tissue & Cell*, 29, 107–118.

Figs 29–37. Sperm of *F. hepatica*, TEM immunocytochemistry: **29.** Longitudinal section of the spermatozoon showing the α-tubulin labelling; scale bar = 0.5 μm. **30.** Longitudinal section of the spermatozoon showing the acetylated-tubulin labelling; scale bar = 0.3 μm. **31.** Cross-sections of the spermatozoon showing the α-tubulin labelling; scale bar = 0.5 μm. **32.** Cross-section of the spermatozoon showing the β-tubulin labelling; scale bar = 0.2 μm. **33.** Cross-section of the spermatozoon showing the acetylated-tubulin labelling; scale bar = 0.2 μm. **34.** Cross-section of the spermatozoon showing the tyrosinated-tubulin labelling; scale bar = 0.3 μm. **35.** Cross-sections of a zone of differentiation, free flagella and median cytoplasmic process showing the α-tubulin labelling; scale bar = 0.5 μm. **36.** Cross-section of the spermatozoon showing the β-tubulin labelling; scale bar = 0.3 μm. **37.** Cross-section of the free flagellum and median cytoplasmic process showing the tyrosinated-tubulin labelling; scale bar = 0.3 μm

Iomini C., Raikova O., Noury-Sraïri N., Justine J.-L. 1995. Immunocytochemistry of tubulin in spermatozoa of Platyhelminthes. *Mémoires du Muséum National d'Histoire Naturelle*, *Paris*, 166, 97–104.

Jamieson B.G.M., Daddow L.M. 1982. The ultrastructure of the spermatozoon of *Neochasmus* sp. (Cryptogonimidae, Digenea, Trematoda) and its phylogenetic significance. *International Journal for Parasitology*, 12, 547–559.

Justine J.-L. 1995. Spermatozoal ultrastructure and phylogeny of the parasitic Platyhelminthes. *Mémoires du Muséum National d'Histoire Naturelle*, *Paris*, 166, 55–86.

Justine J.-L. 1999. Spermatozoa of Platyhelminthes: Comparative ultrastructure, tubulin immunocytochemistry and nuclear labelling. In: *The male gamete*: *From basic science to clinical applications* (Ed. C. Gagnon). Cache River Press, Vienna, Illinois, 351–362.

Justine J.-L., Iomini C., Raikova O., Mollaret I. 1998. The homology of cortical microtubules in platyhelminth spermatozoa: a comparative immunocytochemical study of acetylated tubulin. *Acta Zoologica* (*Stockholm*), 79, 235–241.

Justine J.-L., Mattei X. 1982a. Étude ultrastructurale de la spermiogénèse et du spermatozoïde d'un plathelminthe: *Gonapodasmius* (Trematoda: Didymozoidae). *Journal of Ultrastructure Research*, 79, 350–365.

Justine J.-L., Mattei X. 1982b. Réinvestigation de l'ultrastructure du spermatozoïde d'*Haematoloechus* (Trematoda: Haematoloechidae). *Journal of Ultrastructure Research*, 81, 322–332.

Mas-Coma S., Fons R., Feliu C., Bargues M.D., Valero M.A., Galán-Puchades M.T. 1988. Small mammals as natural definitive hosts of the liver fluke, *Fasciola hepatica* Linnaeus, 1758 (Trematoda: Fasciolidae): A review and two new records of epidemiologic interest on the Island of Corsica. *Rivista di Parassitologia*, 5, 73–78.

Meaney M.I., Fairweather I., Brennan G.P., Ramasamy P., Subramanian P.B. 2002. *Fasciola gigantica*: tegumental surface alterations following treatment *in vitro* with the sulphoxide metabolite of triclabendazole. *Parasitology Research*, 88, 315–325.

Miquel J., Marchand B. 2001. Tubulin immunocytochemistry of the spermatozoa in the cestode *Mesocestoides litteratus* (Mesocestoididae). *Acta Parasitologica*, 46, 130–134.

Miquel J., Nourrisson C., Marchand B. 2000. Ultrastructure of the spermiogenesis and the spermatozoon of *Opecoeloides furcatus* (Trematoda, Digenea, Opecoelidae), a parasite of *Mullus barbatus* (Pisces, Teleostei). *Parasitology Research*, 86, 301–310.

Mollaret I., Justine J.-L. 1997. Immunocytochemical study of tubulin in the 9+'1' sperm axoneme of a monogenean (Platyhelminthes), *Pseudodactylogyrus* sp. *Tissue & Cell*, 29, 699–706.

Ndiaye P.I., Miquel J., Bâ C.T., Feliu C., Marchand B. 2002. Spermiogenesis and sperm ultrastructure of *Scaphiostomum palaearcticum* Mas-Coma, Esteban et Valero, 1986 (Trematoda, Digenea, Brachylaimidae). *Acta Parasitologica*, 47, 259–271.

Ndiaye P.I., Miquel J., Bâ C.T., Marchand B. Ultrastructure of the spermiogenesis and the spermatozoon of the liver fluke *Fasciola gigantica* Cobbold, 1856 (Digenea, Fasciolidae), a parasite of cattle in Senegal. *Journal of Parasitology*, in press.

Ndiaye P.I., Miquel J., Feliu C., Marchand B. 2003. Ultrastructure of the spermiogenesis and spermatozoa of *Notocotylus neyrai* González Castro, 1945 (Digenea, Notocotylidae), intestinal parasite of *Microtus agrestis* (Rodentia: Arvicolidae) in Spain. *Invertebrate Reproduction and Development*, 43, 105–115.

Orido Y. 1988. Ultrastructure of spermatozoa of the lung fluke, *Paragonimus ohirai* (Trematoda: Troglotrematidae), in the seminal receptacle. *Journal of Morphology*, 196, 333–343.

Raikova O.I., Flyatchinskaya L.P., Justine J.-L. 1998. Acoel spermatozoa: ultrastructure and immunocytochemistry of tubulin. *Hydrobiologia*, 383, 207–214.

Raikova O.I., Justine J.-L. 1999. Microtubular system during spermiogenesis and in the spermatozoon of *Convoluta saliens* (Platyhelminthes, Acoela): tubulin immunocytochemistry and electron microscopy. *Molecular Reproduction and Development*, 52, 74–85.

Rees F.G. 1979. The ultrastructure of spermatozoon and spermiogenesis in *Cryptocotyle lingua* (Digenea: Heterophyidae). *International Journal for Parasitology*, 9, 405–419.

Reynolds E.S. 1963. The use of lead citrate at high pH as an electron-opaque stain in electron microscopy. *Journal of Cell Biology*, 17, 208–212.

Robinson M.W., Colhoun L.M., Fairweather I., Brennan G.P., Waite J.H. 2001. Development of the vitellaria of the liver fluke, *Fasciola hepatica* in the rat host. *Parasitology*, 123, 509–518.

Srimuzipo P., Komalamisra C., Choochote W., Jitpakdi A., Vanichthanakorn P., Keha P., Riyong D., Sukontasan K., Komalamisra N., Sukontasan K., Tippawangkosol P. 2000. Comparative morphometry, morphology of eggs and adult surface topography under light and scanning electron microscopies, and metaphase karyotype among three size-races of *Fasciola gigantica* in Thailand. *Southeast Asian Journal of Tropical Medicine and Public Health*, 31, 366–373.

Stitt A.W., Fairweather I. 1990. Spermatogenesis and the fine structure of the mature spermatozoon of the liver fluke, *Fasciola hepatica* (Trematoda: Digenea). *Parasitology*, 101, 395–407.

Stitt A.W., Fairweather I. 1992. Spermatogenesis in *Fasciola hepatica*: an ultrastructural comparison of the effects of the anthelminthic, triclabendazole ("Fasinex") and the microtubule inhibitor, tubulozole. *Invertebrate Reproduction and Development*, 22, 139–150.

Tang J.-Y., Wang W., Wang G. 1998. Studies on ultrastructure of spermatogenesis and sperm in *Pseudorhipidocotyle elpichthys*. *Acta Hydrobiologica Sinica*, 22, 168–173.

(Accepted July 7, 2003)